M. A. Fayazbakhsh
Laboratory for Alternative Energy Conversion,
School of Mechatronic Systems Engineering,
Simon Fraser University,
250-13450 102 Avenue,
Surrey, BC V3T 0A3, Canada

F. Bagheri
Laboratory for Alternative Energy Conversion,
School of Mechatronic Systems Engineering,
Simon Fraser University,
250-13450 102 Avenue,
Surrey, BC V3T 0A3, Canada

M. Bahrami[1]
Laboratory for Alternative Energy Conversion,
School of Mechatronic Systems Engineering,
Simon Fraser University,
250-13450 102 Avenue,
Surrey, BC V3T 0A3, Canada
e-mail: mbahrami@sfu.ca

A Self-Adjusting Method for Real-Time Calculation of Thermal Loads in HVAC-R Applications

A significant step in the design of heating, ventilating, air conditioning, and refrigeration (HVAC-R) systems is to calculate room thermal loads. The heating/cooling loads encountered by the room often vary dynamically while the common practice in HVAC-R engineering is to calculate the loads for peak conditions and then select the refrigeration system accordingly. In this study, a self-adjusting method is proposed for real-time calculation of thermal loads. The method is based on the heat balance method (HBM) and a data-driven approach is followed. Live temperature measurements and a gradient descent optimization technique are incorporated in the model to adjust the calculations for higher accuracy. Using experimental results, it is shown that the proposed method can estimate the thermal loads with higher accuracy compared to using sheer physical properties of the room in the heat balance calculations, as is often done in design processes. Using the adjusted real-time load estimations in new and existing applications, the system performance can be optimized to provide thermal comfort while consuming less overall energy. [DOI: 10.1115/1.4031018]

Keywords: HVAC-R, thermal loads, real-time calculation, self-adjusting method, heat balance method

1 Introduction

A significant portion of the worldwide energy is consumed by HVAC-R systems. The energy consumption by HVAC-R systems is 50% of the total energy usage in buildings and 20% of the total national energy usage in European and American countries [1]. HVAC-R energy consumption can exceed 50% of the total energy usage of a building in tropical climates [2]. Furthermore, refrigeration systems also consume a substantial amount of energy. Supermarket refrigeration systems, as an example, can account for up to 80% of the total energy consumption in the supermarket [3].

Vehicle fuel consumption is also significantly affected by air conditioning. The HVAC-R energy usage in a typical vehicle outweighs the energy loss to rolling resistance, aerodynamic drag, and driveline losses. HVAC-R systems can reduce the fuel economy of midsized vehicles by more than 20% while increasing NO_x and CO emissions by approximately 80% and 70%, respectively [4]. Moreover, HVAC-R is a critical system for hybrid electric vehicles and electric vehicles, as it is the second most energy consuming system after the electric motor [5]. The energy required to provide cabin cooling for thermal comfort can reduce the range of plug-in electric vehicles by up to 50% depending on outside weather conditions [4]. Less energy consumption by mobile HVAC-R systems directly results in higher mileage and better overall efficiency on the road.

Proper design and efficient operation of any HVAC-R system require: (i) accurate calculation of thermal loads and (ii) appropriate design and selection of the HVAC-R system. The common practice among HVAC-R engineers is to begin by estimating the room thermal loads. This step consists of a careful study of the room characteristics such as wall properties, fenestration, openings, and air distribution. The room usage pattern, occupancy level, geographical location, and ambient weather conditions are other necessary data that need to be thoroughly investigated before a decision is made on the design cooling/heating load. An HVAC-R system that can handle the calculated load is then selected. As such, much detailed information is required in order to properly calculate the thermal loads and select the system. Innovative methods that can accurately calculate instantaneous thermal loads without requiring a hefty amount of details can be promising in the design of new HVAC-R systems.

On–off and modulation controllers are widely used in HVAC-R systems, which use the room temperature as the controlled variable [6]. However, such controllers mostly act upon the current temperature value and are not aware of the actual thermal load and its variation pattern over the duty cycle. It is shown that intelligent control of the HVAC-R operation based on thermal load prediction can help maintain air quality while minimizing energy consumption [7,8]. By predicting the thermal loads in real-time, controllers are enabled to not only provide thermal comfort in the current condition but also adjust the system operation to cope with upcoming conditions in an efficient manner. Having real-time estimation of thermal loads can result in improved energy efficiency, as the HVAC-R system is enabled to adapt to various demand situations. Arguello-Serrano and Velez-Reyes [9] stated that availability of thermal load estimations efficiently allows the HVAC-R controller to provide comfort regardless of the thermal loads. Afram and Janabi-Sharifi [10] showed that improved load estimations can lead to the design and testing of more advanced controllers. Zhu et al. [11] studied an optimal control strategy for minimizing the energy consumption using variable refrigerant flow and variable air volume air conditioning systems. Qureshi and Tassou [12] reviewed various methods of capacity control in refrigeration systems and stated that using variable-speed compressors can be the most energy-efficient method for capacity

[1]Corresponding author.

Contributed by the Heat Transfer Division of ASME for publication in the Journal of Thermal Science and Engineering Applications. Manuscript received March 20, 2015; final manuscript received June 8, 2015; published online July 28, 2015. Assoc. Editor: Zahid Ayub.

control. Therefore, the ability to accurately predict thermal loads in real-time can improve the feedback information for the control of HVAC-R systems, which in turn results in significant reduction of total energy consumption and greenhouse gas emissions.

The literature is rich with various approaches proposed for calculation of thermal loads. The American Society of Heating, Refrigerating, and Air Conditioning Engineers (ASHRAE) recognize some of them including the HBM [13]. HBM is a straightforward and rigorous method that involves calculating a surface-by-surface heat balance of the surrounding walls of the room through consideration of conductive, convective, and radiative heat transfer mechanisms. After calculation of heat flows across all walls and openings, the heat balance equation is solved for the room air to complete the solution procedure. The method has been extensively used in residential, nonresidential, and mobile applications [14–17].

HBM is known as a "forward" or "law-driven" approach, i.e., it estimates the loads based on rigorous details of the room. Feedback data from the system are seldom incorporated in the formulations of this method. In contrast to HBM, "inverse" or "data-driven" methods study existing HVAC-R systems and allow the thermal performance of the system to be inferred from measured temperature values. Such approaches mathematically evaluate the loads through learning and testing rather than analyzing the heat transfer equations. Li et al. [18] presented four modeling techniques for hourly prediction of thermal loads. The methods included back propagation neural network, radial basis function neural network, general regression neural network, and support vector machine. The mathematical models they used correlated the cooling load with parameters such as the ambient weather, but the heat transfer equations were not explicitly used. Kashiwagi and Tobi [19] also proposed a neural network algorithm for prediction of thermal loads. Ben-Nakhi and Mahmoud [20] used general regression neural networks and concluded that a properly designed neural network is a powerful tool for optimizing thermal energy storage in buildings based only on external temperature records. They claimed that their set of algorithms could learn over time and improve the prediction ability. Sousa et al. [21] developed a fuzzy controller to be incorporated as a predictor in a nonlinear model-based predictive controller. Yao et al. [22] used a case study to show that a combined forecasting model based on a combination of neural networks and a few other methods can be promising for predicting a building's hourly load for the future hours. Solmaz et al. [23] used the same concept of neural networks to predict the hourly cooling load for vehicle cabins. Fayazbakhsh et al. [24] proposed a simple method that can estimate the total heat gain and thermal inertia of the room using an inverse calculation method and real-time temperature measurements.

Although producing acceptable results, methods that are purely based on artificial intelligence are inherently unaware of the heat transfer mechanisms. Thus, they might prove unreliable in new scenarios and conditions for which they are not trained. A number of recent studies aim at combining artificial intelligence algorithms with conventional load calculation methods to improve them. For instance, Wang and Xu [25,26] used genetic algorithm to estimate thermal parameters of a building thermal network model using the operation data collected from site monitoring. They combined a resistance–capacitance (RC) model of the building envelope with a data-driven approach where their RC model parameters were corrected via real-time measurements. The results of conventional load calculation methods can be improved by incorporating new mathematical algorithms that act on simple real-time measurements.

Table 1 summarizes the above-mentioned studies proposing novel methods for calculation of thermal loads for various applications. The disadvantage of some of these methods is their complexity of implementation in typical HVAC-R applications. While relying upon conventional design methods can cause remarkable inaccuracies in thermal load estimations, incorporation of artificial intelligence methods may require computational resources that may not be available for typical systems. An accurate real-time load calculation method that is also simple to implement can be beneficial for practical engineering applications of HVAC-R design.

In this study, the HBM is combined with a data-driven approach to propose a new model for thermal load estimation. The proposed method is based on the governing equations of heat transfer while utilizing real-time measurements to improve the estimation accuracy. A simple mathematical approach based on gradient descent optimization is used to adjust the method's coefficients during a few training steps. The proposed method is intended to be an intermediate solution for simple yet accurate thermal load calculations. In comparison to the above-mentioned studies, it is attempted that the current method be:

- based on fundamental heat transfer equations, therefore generally applicable to various problems, but requiring little room information,
- data-driven, therefore automatically adjusted based on feedback temperatures, but requiring few sensors, and
- mathematically simple, therefore avoiding computational intensity, but providing accurate load calculations.

A testbed is designed and built to simulate thermal loads in a generic chamber. The modeling results are experimentally validated using the testbed. The approach can aid the design process of new systems and also help retrofit existing systems. The main advantage of the proposed method is that it can provide controllers with an estimation of the real-time thermal loads, while the accuracy of the method is progressively improved by a mathematical self-adjusting algorithm. Moreover, the present model is relatively simple and computationally inexpensive. Since the general form of the HBM is used as the basis for the governing equations, the proposed method is applicable to any HVAC-R system in

Table 1 Summary of studies proposing novel methods to calculate HVAC-R thermal loads for various applications

Authors	Application	Method
Khayyam et al. [7,8,17,37]	Automotive	Fuzzy predictive control
Barnaby et al. [14]	Residential building	HBM
Fayazbakhsh and Bahrami [15]	Automotive	HBM
Arici et al. [16]	Automotive	Analytical energy balance
Li et al. [18]	Office building	Support vector machine and artificial neural network
Kashiwagi and Tobi [19]	Residential building	Artificial neural network
Ben-Nakhi and Mahmoud [20]	Office building	General regression neural network
Yao et al. [22]	Office building	Analytic hierarchy process
Solmaz et al. [23]	Automotive	Artificial neural network
Sousa et al. [21]	Generic	Fuzzy predictive control
Fayazbakhsh et al. [24]	Freezer room	HBM
Wang and Xu [25,26]	Office building	Genetic algorithm
Zhai et al. [27–32]	Building	CFD

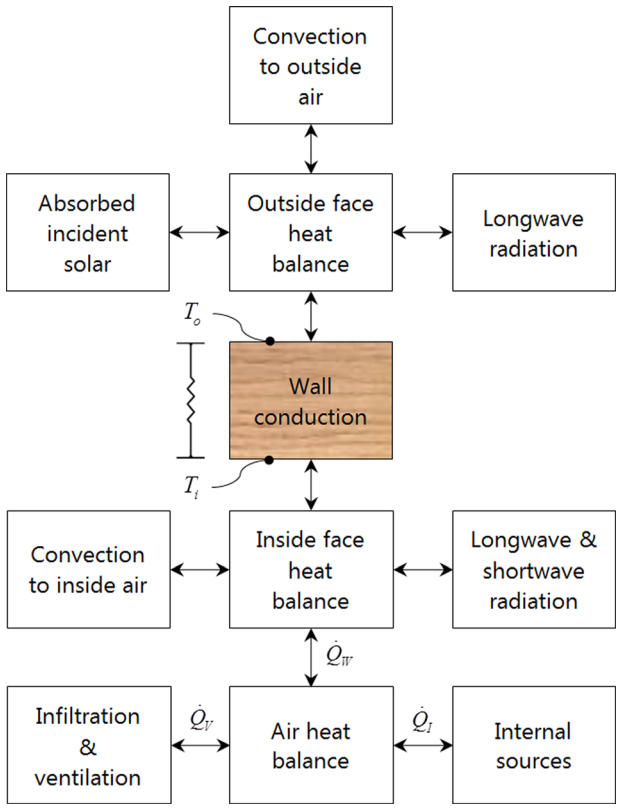

Fig. 1 Schematic of the HBM [13]. Each wall is represented by a conductive resistance for steady-state conditions. T_i and T_o represent the temperatures on the inside and outside surfaces of the wall.

general. As such, the same concept can be used for residential buildings, office buildings, freezer rooms, and vehicle air conditioning systems.

2 Model Development

The methodology of the HBM is followed to develop a real-time thermal load calculation algorithm. As shown at the bottom of Fig. 1, the room air is in thermal balance with internal sources, ventilation load, and heat transfer across walls, as shown by the following equation:

$$\dot{Q}_I = \dot{Q}_V + \dot{Q}_W \tag{1}$$

where $\dot{Q}_V$ is the heat loss due to ventilation and infiltration, $\dot{Q}_W$ is the total heat loss from the room to the ambient air across the walls, and $\dot{Q}_I$ is the heat gain from internal sources. In the absence of a cooling system and when the steady-state condition is reached, i.e., when all temperatures are relatively constant, the room is in thermal balance and Eq. (1) formulates the zone air heat transfer.

The calculation of $\dot{Q}_W$ consists of three steps: (a) outside face heat balance, (b) conduction through the wall, and (c) inside face heat balance. The heat balances on the interior and exterior wall faces occur through radiation and convection mechanisms. As shown in Fig. 1, both longwave and shortwave radiations can occur on the interior and exterior surfaces. Moreover, the radiation can originate from transmitted solar rays or radiation exchange with other zone surfaces. The bulk of the radiation energy received at each surface contributes to the temperature increase at that surface. Heat is then transferred to the inside or outside air through the convection mechanism. Thus, the total wall heat loss $\dot{Q}_W$ in Eq. (1) consists of the total heat transfer across all walls through all possible mechanisms of heat transfer including radiation, conduction, and convection.

The convection and radiation mechanisms depend on various factors such as wall orientation and shape as well as adjacent air velocity and temperature. Finding the proper convective coefficient and linearized radiative coefficient requires correlations that may not hold for all conditions, especially in vehicle applications. As an instance of the importance of this issue, the studies by Zhai et al. [27–32] are noteworthy. They developed an entire methodology to couple computational fluid dynamics (CFD) simulations with energy simulations to improve the accuracy of the latter for various air distribution patterns and convective coefficients. Of course, such methods are time consuming and computationally intensive and may not be desirable options for many applications, especially on board a vehicle. Thus, the calculation of the convective and radiative heat transfer rates intrinsically contains more complexity compared to the conductive heat transfer which follows the Fourier's law of conduction [33].

The wall conduction is in series to the outside and inside face heat balances, i.e., the same amount of heat transfer rate crossing the outside face, conducts through the wall, and eventually passes through the inside face. Having a real-time measurement of the temperatures on both sides of a wall, i.e., having the actual T_o and T_i at steady-state conditions enables us to calculate the total heat transfer rate across the wall.

The total wall heat transfer rate is the summation of all individual wall heat transfer values

$$\dot{Q}_W = \sum_{j=1}^{n} \dot{Q}_{W,j} \tag{2}$$

where $\dot{Q}_{W,j}$ is the heat transfer rate across wall j and n is the number of walls. According to Fourier's law of conduction [33], the heat transfer rate is linearly related to the temperature gradient

$$\dot{Q}_{W,j} = \left(\frac{kA}{b}\right)_j (T_i - T_o)_j \tag{3}$$

where k is the conduction heat transfer coefficient, A is the wall surface area, and b is the wall thickness. The underlying assumptions for using Eq. (3) are uniform temperature over the surface, uniform wall thickness, and uniform thermal conductivity. In practice, rarely any of these conditions are met. The wall of a vehicle cabin or a residential room normally has different layers of materials with various thicknesses and thermal properties. Furthermore, much geometrical and thermal information are either unavailable or inaccurate while analyzing or retrofitting the HVAC-R performance of a room. An adjustment method is proposed in the following text to automatically calculate and correct the wall heat transfer coefficients.

Combining Eqs. (2) and (3), the total wall heat transfer rate is written as

$$\dot{Q}_W = \sum_{j=1}^{n} \left(\frac{kA}{b}\right)_j (T_i - T_o)_j \tag{4}$$

$\dot{Q}_V$ is caused by the movement of air in or out of the zone and its calculation is thus more complicated than the conductive heat transfer mechanism. On the other hand, natural convection and forced convection of air through openings and seams are inevitable in many practical cases. Thus, we assume a constant steady-state value to represent the ventilation heat transfer rate. Replacing $w_0 = \dot{Q}_V$ and $w = kA/b$ in Eqs. (1) and (4), we arrive at

$$\dot{Q}_I = \dot{Q}_V + \dot{Q}_W = w_0 + \sum_{j=1}^{n} w_j (T_i - T_o)_j \tag{5}$$

where $w_0 - w_n$ are called the weight factors. As previously mentioned, there are always uncertainties and inaccuracies associated with the calculation of the weight factors. Nevertheless, considering Eq. (1) for steady-state conditions, if $\dot{Q}_I$ and the temperatures T_i and T_o are known for a few cases, a gradient descent optimization technique can be utilized to adjust the weight factors progressively and use the adjusted weights for future load calculations. This approach leads to a self-adjusting algorithm for the real-time calculation of the wall heat transfer rates.

Equation (5) is a linear function in which w_0 is called the "bias weight" and $w_1 - w_n$ are called the "input weights" [22,34–36]. In order to establish a simple formula for updating the weight factors, a "transfer function" f can be applied to the right-hand side of Eq. (5) to arrive at the following:

$$O = f\left(w_0 + \sum_{j=1}^{n} w_j (T_i - T_o)_j\right) \tag{6}$$

where O is the calculated output and f is the sigmoid function [36]

$$f(x) = \frac{1}{1 + \exp(-x)} \tag{7}$$

Finally, in order to adjust the weight factors $w_0 - w_n$, a training process is required where $\dot{Q}_I$ is known alongside the measured temperatures T_i and T_o for a few cases. The correction procedure is implemented according to [34]

$$w_j^{m+1} = w_j^m + \eta (D - O)^m (T_i - T_o)_j^m \tag{8}$$

where η is the learning rate. $D = f(\dot{Q}_I)$ is the desired output found from the known $\dot{Q}_I$ values of the training phase and m denotes the step number of the training algorithm. The set of weight factors found by the training algorithm is eventually inserted in Eq. (5) to arrive at the real-time thermal load for future cases where the direct heat gain from internal sources is unknown. Note that the original equation of heat balance in Eq. (1) is written for steady-state conditions. As such, the training scheme of Eq. (8) is most reliably applicable to temperature measurements at steady-state conditions. In practice, once the steady-state condition is reached, the temperatures are sensed at every time step, say every second, and the training procedure is performed using those readings. However, although the mentioned steps occur in time, they are merely regarded as iteration steps for Eq. (8). Therefore, the overall algorithm must not be mistaken for a transient formulation.

In summary, the objective function of the discussed optimization algorithm is $F = |D - O|$, which is the difference between the real internal heat gain and the calculated internal heat gain. Although the weight factors may mathematically converge to negative values, it is necessary that they retain their physical meaning, i.e., the wall thermal conductance values, which are always positive. Thus, it is deemed to minimize the objective function F subject to the constraints $w_0, w_1, \ldots, w_n > 0$. A significant advantage of the proposed technique is that considerably little information need to be known about the room in order to calculate the thermal loads. The weight factors which are updated in the training procedure can be initiated from any arbitrary value such as zero.

Figure 2 summarizes the overall load calculation algorithm including the training procedure. As shown in Fig. 2, the weight factors are updated in the training procedure until their relative variation is smaller than a selected convergence criterion ε. Once the weight factors have converged within the selected range of error, they can be used to estimate $\dot{Q}_V + \dot{Q}_W$ in the future conditions when $\dot{Q}_I$ is unknown.

The model is deemed to be used for improved calculation of thermal loads. It is based on the HBM, but the necessary

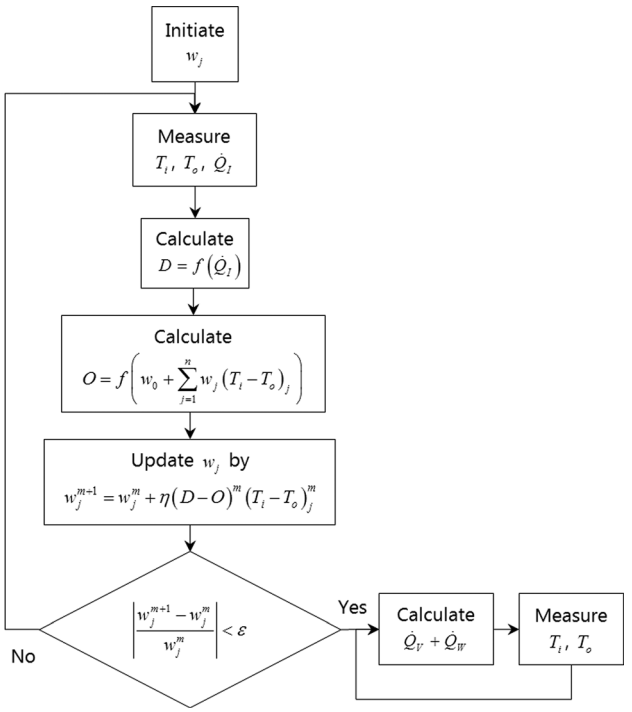

Fig. 2 Flowchart of the self-adjusting algorithm for real-time calculation of thermal loads by automatic estimation of conduction coefficients

coefficients used in that method are adjusted by a gradient descent optimization technique. Intelligent algorithms can be applied to various design stages: (1) thermal load calculations, (2) refrigeration system control, and (3) tuning controller parameters. Li et al. [18] used several techniques based on neural networks in order to calculate the thermal loads (stage 1). In such methods, the mathematical formulations are not based on heat transfer formulae and the algorithm attempts to correlate between the thermal load and its affecting parameters unaware of the underlying governing equations. Some studies by Khayyam et al. [7,8] used a law-driven methods to calculate the loads in the first stage, but developed a novel controller based on a combination of neural network and fuzzy controller in the next stage (stage 2). In another study, Khayyam et al. [37] used a law-driven approach for thermal load calculation alongside a proportional-integral-derivative (PID) controller, but used neural networks to tune the PID gains and achieve energy efficiency (stage 3). The approach pursued in this study aims to utilize the HBM for thermal load calculations (stage 1), while the gradient descent optimization technique is utilized to improve the accuracy. The thermal load estimation data provided by this method can aid conventional or intelligent controllers to streamline the operation of the HVAC-R system.

3 Results and Discussion

To test and verify the proposed model, a custom-designed testbed is built as shown in Fig. 3. The testbed is built out of wooden, plastic, and glass materials and is adjustable for different dimensions and angles to mimic the cabin of a sedan car. Six pairs of T-type thermocouples (5SRTC-TT-T-30-36, Omega Engineering, Inc., Laval, QC, Canada) are attached on the chamber walls, each pair connected to the two sides of a wall at the same spot. The thermocouples have a tolerance of $\pm 1.0°C$ and are connected to a data acquisition system (NI 9214DAQ, National Instruments Canada, Vaudreuil-Dorion, QC, Canada) for collecting the temperature values at a sampling rate of 1Hz. Regular tape was used to attach the thermocouples, as shown in Fig. 3. Since the present

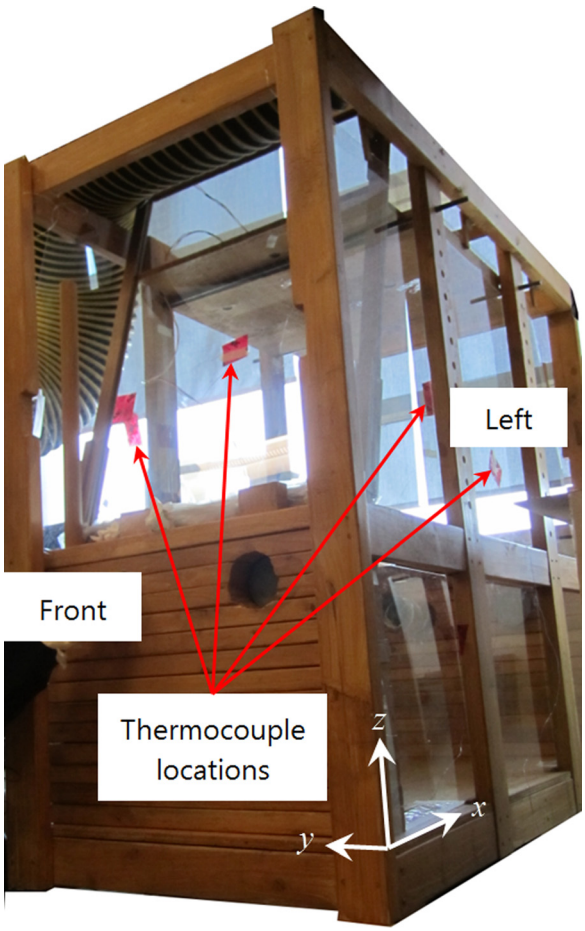

Fig. 3 A picture of the testbed used for implementing the present model. Six thermocouple pairs are attached on the testbed walls. Each pair consists of two thermocouples attached on the opposite sides (inside and outside) of the wall.

model relies on automatic adjusting of the wall heat transfer coefficients, no specific concern exists regarding the accurate location and attachment method of the thermocouples. There are four openings on the front and rear walls of the chamber which are all blocked and the chamber is sealed in order to avoid air infiltration and ventilation. However, a small amount of air infiltration may still exist due to imperfect air sealing.

Table 2 shows the precise locations of the installed thermocouples. The reference coordinates are shown in Fig. 3. Each pair consists of two opposing thermocouples installed on the two opposite sides of the corresponding wall in the chamber. Figure 4 shows a computer model of the chamber alongside its cross section in a cut view. Overall chamber dimensions are also shown in Fig. 4, and the names of different components and parts are also identified.

An electrical heater with controlled input power is placed inside the chamber at an arbitrary location. A fan is placed behind the heater to blow air over it and properly circulate warm air inside the chamber. The location of the fan is kept constant for all tests, since a new air distribution pattern might necessitate retraining the algorithm to update the weight factors. While the heater power is variable, the fan power consumption is constant and measured as 10W. This energy consumption is eventually converted to heat in the enclosed chamber through damping of the air motion. Therefore, this value is also added to the total heating power. The heater consists of a resistor that provides Joule heating with controlled input power. The amount of power provided to the heater is controlled and monitored by a programmable DC power supply (62000P, Chroma Systems Solutions, Inc., Orange County, CA). According to the manufacturer's datasheet, the uncertainty of the power consumption measurements is 0.4%. Since there is no other heat source available in the chamber, the total power input to the fan and the heater can be regarded as the direct heat gain from internal sources $\dot{Q}_I$ of Eq. (1).

Table 2 Locations of thermocouple pairs installed on the testbed walls. Refer to Fig. 3 for reference coordinates.

Thermocouple pair name	x (cm)	y (cm)	z (cm)
Front	10.4	37.5	138.6
Rear	147.1	37.5	148.3
Left	80.0	0.0	85.0
Right	35.0	75.0	100.0
Top	55.0	55.0	130.7
Bottom	55.0	65.0	0.0

The model is applied to the testbed shown in Fig. 3 for various values of direct internal heat gain enforced by varying heater power levels. At every stage, the heater power is kept constant for 10 min in order to assure the steady-state condition is reached. Figure 5 shows the temperature values at the steady-state conditions reached after 10 min for every level of total heat gain. The heater power is varied from $\dot{Q}_I = 0.235$ kW to $\dot{Q}_I = 0.460$ kW covering 30 discrete levels. The average value of the six interior thermocouples is shown as the inside average temperature, and the average of the six exterior thermocouple measurements is shown as the outside average temperature. The average temperatures increase with the heat gain while the gap between the inside and outside temperatures increases as well, signifying an increase in the overall heat transfer across the walls. The temperature gradients $(T_i - T_o)$ are all positive, which demonstrates that heat is being lost to the ambient air in this heating scenario. The value and rate of increase of temperature gradients are different for different walls. The top and bottom plates are much thicker than the surrounding walls, creating a higher thermal resistance. As a result, as observed for the top and bottom plates, higher temperature gradients are inevitable for conducting the same heat flow rate. Moreover, for the heating scenario tested, natural convection causes higher heat transfer at the top compared to the bottom plate, creating an even higher temperature gradient at the top. The weight factors, once trained and adjusted, automatically assign the importance or "weight" of each wall in the overall thermal load to provide reliable estimations based on real-time temperature measurements.

In order to use the proposed method for estimation of thermal loads, the training algorithm is applied on the weight factors for 20 steps at an arbitrary heater power setting of $\dot{Q}_I = 0.334$ kW. After reaching the steady state, i.e., when all temperatures are almost constant within $\pm 0.5\,^{\circ}$C, the training procedure is initiated by feeding the real-time temperatures to the algorithm and adjusting the weight factors accordingly. One temperature measurement is performed per second and Eq. (8) is solved at every step using $D = f(0.334)$. A learning rate of $\eta = 0.05$ is used. Having arbitrarily initiated from $w_0, w_1, \ldots, w_n = 0$, Fig. 6 shows the progressive adjustment of the weight factors and the calculated heat gain. Since the training procedure is an initial-condition iterative algorithm, the converged set of weight factors is dependent on the initial guess. However, in order to ensure that the resulting set of weight factors is correct for all future loading conditions, it is recommended to repeat the training algorithm for several heat gain conditions.

To validate the model, the testbed wall thermal conductance values are measured. A thermal conductivity measurement machine (Hot Disk TPS 2500 S Thermal Conductivity System, ThermTest, Inc., Fredericton, NB, Canada) is used to measure the thermal conductivity k of the chamber components. The thermal conductivity of the glass, wood, and plastic materials used for constructing the chamber is measured as 1.05 W/m °C, 0.2 W/m °C, and 0.26 W/m °C, respectively. As observed in

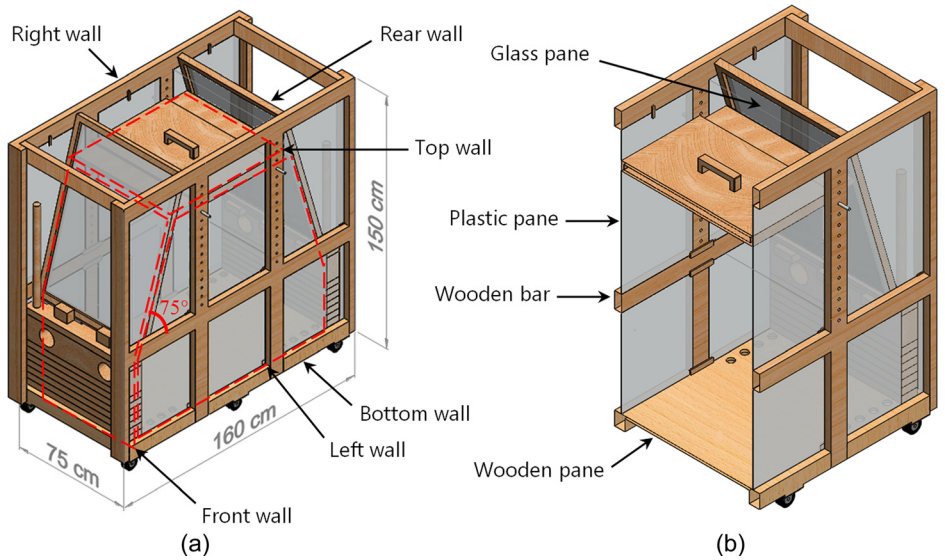

Fig. 4 Computer model of the testbed showing its overall dimensions and components: (*a*) full chamber model and (*b*) cut view showing the chamber's cross section

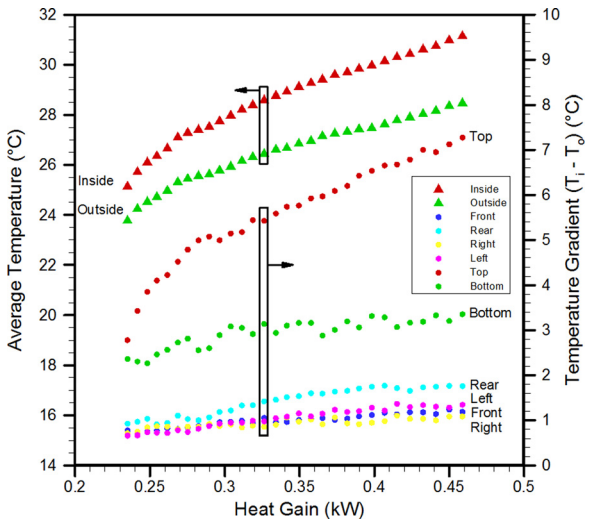

Fig. 5 Average inside and outside temperatures (left axis) and temperature difference between inside and outside wall surfaces ($T_i - T_o$) (right axis) for various levels of controlled internal heat gain in the testbed

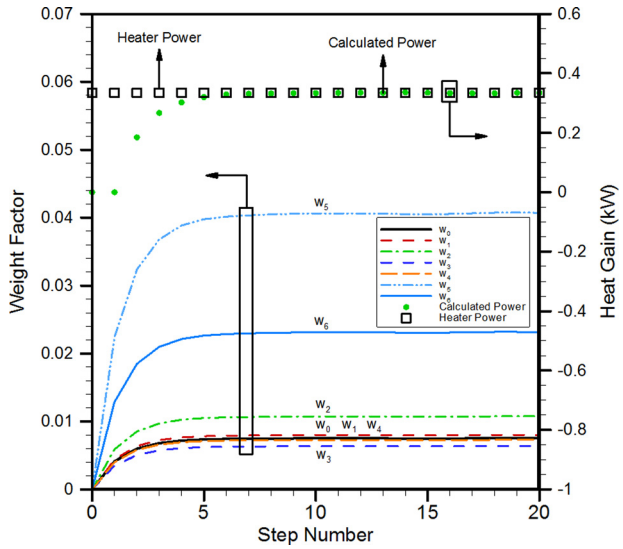

Fig. 6 Progressive training of weight factors and calculated heat gain for an arbitrary heat gain of $\dot{Q}_l = 0.334$ kW. The weight factors are adjusted based on real-time temperature measurements and the known heat gain.

Fig. 3, the chamber walls do not consist of uniform materials. Furthermore, the wall shapes are not necessarily flat and their thicknesses are nonuniform. Table 3 shows an approximate average of the thicknesses, surface areas, and overall heat transfer coefficients of the testbed walls.

In common engineering practice, the designer would investigate the room and find the conductance values shown in Table 3 to be used in the HBM and Eq. (4). If the conductance values found from the careful measurement of thickness, area, and conductivity are precise, they will satisfy the heat balance equation and accurate load calculations will follow. However, accurate material data are seldom available to be used in precise estimations of conductance values. Furthermore, wall materials and insulations are often subject to degradation, which changes their conductivity value. Moreover, the averaging and approximation of the properties by the engineer are prone to inaccuracies that can result in thermal load miscalculations. The current method provides a means to overcome these issues by utilizing actual system data for calculation adjustment. The proposed method can thus be specifically promising for retrofitting existing systems and designing new ones.

Table 4 shows the adjusted weight factors after 20 correction steps shown in Fig. 6. Note that all the weight factors are initiated from zero, which means that the method can perform well almost unsupervised. As observed in Fig. 6, the calculated power is converged to the exact heater power in seven steps, i.e., after only 7 s of training. It shows that a controller designed based on the proposed algorithm can adjust to the room conditions within seconds of the training procedure initiation.

Since the gradient descent optimization technique inherently finds the local minima of the objective function [38], the adjusted weight factors depend on their initial values and can converge to a combination of $w_0 - w_6$ that may not necessarily correspond to the global minimum of the objective function. As such, a disadvantage of the proposed method is that the weight factors may converge to wrong values and the training algorithm can get trapped in local minima. Bad convergence may result in incorrect

Table 3 Approximate average thicknesses, surface areas, and overall heat transfer coefficients of testbed walls. Refer to Fig. 4 for component names and locations.

Wall name	Surface area $A(m^2)$	Thickness $b(mm)$	Heat transfer coefficient $kA/b(kW/°C)$
Front	0.5	5.5	0.095
Rear	0.5	5.5	0.095
Left	2.0	2.0	0.260
Right	2.0	2.0	0.260
Top	2.0	30.0	0.013
Bottom	3.0	30.0	0.020

load estimations at heat gain levels other than what the algorithm is trained for. Also, a change in the air distribution pattern can lead to uselessness of the old trainings. In order to avoid such issues, it is recommended that the algorithm be trained as many times as possible during the system operation. By random triggering of the training procedure over the lifetime of the HVAC-R system, the risk of load miscalculations can be minimized.

The testbed wall properties are carefully investigated to acquire the wall conductance values as accurately as possible. However, all the weight factors shown in Fig. 6 have converged to different values than their physical estimations in Table 3. Table 4 shows the adjusted weight factors compared to their physical estimation according to their corresponding heat transfer coefficients shown in Table 3. The relative errors between the adjusted value and physical estimations are shown as the adjustment percentage. It can be inferred from these percentages that the average wall heat transfer coefficients can be estimated with large errors, while utilizing the proposed data-driven approach does not even necessitate any knowledge of the room physical properties.

Figure 7 shows the calculation of thermal loads using both physically estimated and mathematically adjusted weight factors. The 30 discrete levels of internal heat gain discussed in Fig. 5 are tested until the testbed reached the steady state. The thermal load estimation based on the raw physical weight factors is shown as the unadjusted calculation. The heat gain calculations based on the adjusted weight factors are also shown in Fig. 7 as the adjusted calculation. It can be seen that using the raw heat transfer coefficients can result in huge errors in the calculation of thermal loads. In this specific case, there is a minimum of 144% error in the heat gain estimation using physical coefficients. The adjusted weight factors, however, result in a maximum error of 16% in thermal load calculations. It is further observed in Fig. 7 that the adjusted heat gain calculations are relatively more accurate for heater power levels closer to $\dot{Q}_I = 0.334$ kW compared to lower and higher power levels. This hints that the best practice is to train the algorithm for heat gain levels that are more frequently experienced by the system, so that the future estimations will be done more accurately.

The modeling approach of the present study is based on the HBM, which is a general-purpose methodology for residential and nonresidential applications. Since the underlying heat transfer

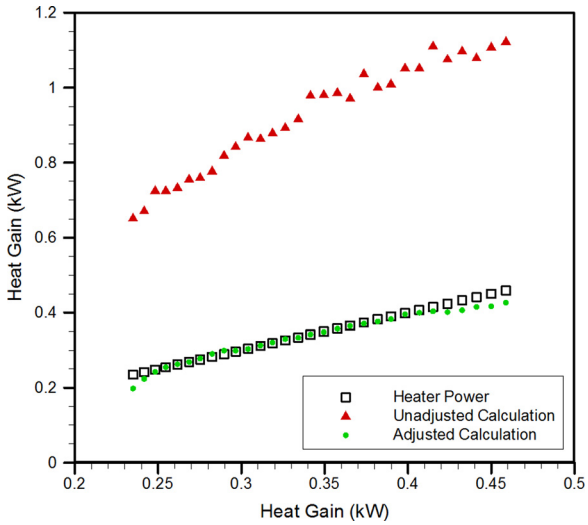

Fig. 7 Calculated steady-state heat gain for different heater power levels based on measured physical values as well as adjusted values of the weight factors

equations are applicable to any geometry and configuration, there is no theoretical hindrance for using it in buildings or vehicles. Therefore, the proposed method can be applied to any stationary, mobile, air conditioning, or refrigeration application. However, since the steady-state conditions are assumed, rapid temperature dynamics may reduce the accuracy of the method. As such, the algorithm must be utilized more cautiously in vehicle applications where the cabin is small and subject to temperature fluctuations.

As a data-driven method, a disadvantage of the proposed method is that it requires some training. Although the training procedure can be performed within seconds, the actual heat gain values which are the training target may be unavailable in many cases, as they can never be directly measured. However, it is possible to artificially impose a known heat gain to an existing room using the same testing approach of this study, i.e., isolating the room from all possible thermal loads except a known source of internal heating or cooling. As such, retrofit analysis of existing systems as well as design of new systems is possible by this method. Whenever direct testing of the room for training is not possible, conventional law-driven methods established by ASHRAE or complicated intelligent algorithms based on fuzzy logic or neural networks can be used to provide an estimation of the actual heat gains. The heat gain values acquired from such methods can be fed to the algorithm to complete the training procedure. Afterward, the proposed algorithm can replace those complicated and time-consuming calculations, as it keeps providing real-time estimations that may be even more accurate than the mentioned methods. Of course, higher accuracy of the law-driven estimations used for training and higher number of installed sensors can directly lead to better performance of the method. Once a system is initiated and trained, the method can

Table 4 Adjusted weight factors compared to their physical estimations, i.e., the approximate heat transfer coefficients. The adjustment percentage shows the relative error between the adjusted and physical values.

Weight factor	Physical interpretation	Physical estimation	Adjusted value	Adjustment percentage (%)
w_0	Ventilation and infiltration	NA	0.0074	NA
w_1	Front wall	0.0950	0.0078	92
w_2	Rear wall	0.0950	0.0106	89
w_3	Left wall	0.2600	0.0063	98
w_4	Right wall	0.2600	0.0072	97
w_5	Top wall	0.0130	0.0402	209
w_6	Bottom wall	0.0200	0.0229	14

be further used for prediction of loads in future cases experienced by the room.

4 Conclusions

A self-adjusting method is proposed to calculate instantaneous thermal loads using real-time temperature measurements. The HBM is incorporated in an automatic correction algorithm, where the gradient descent optimization technique is used for adjusting the heat transfer coefficients. The proposed method is verified by experimental results and it is shown by a case study that the self-adjusting algorithm can estimate the loads with a maximum error of 16% while using the unadjusted physical properties of the walls can lead to a minimum error of 144% in load calculations.

Since the present methodology is based on fundamental heat transfer equations, it can theoretically be used in various applications of stationary, mobile, air conditioning, or refrigeration systems. However, it must be used more cautiously in applications where temperatures are transient and fluctuating. A disadvantage of the proposed method is that it requires some training that may not be readily possible in some applications. To circumvent this issue, other approaches of law-driven load calculation can be utilized as an interim training step. The proposed method can be implemented in existing as well as new HVAC-R systems to aid their design process and retrofit analysis.

Acknowledgment

This work was supported by Automotive Partnership Canada (APC), Grant No. NSERC APCPJ/429698-11. The authors would like to thank the kind support of the Cool-It Group, 100-663 Sumas Way, Abbotsford, BC, Canada. The authors wish to acknowledge David Sticha for his efforts in building the testbed.

Nomenclature

A = surface area (m^2)
b = thickness (m)
D = desired output
f = sigmoid function
F = objective function
k = thermal conductivity (W/m °C)
O = calculated output
$\dot{Q}$ = heat transfer rate (W)
T = temperature (°C)
w = weight factor

Greek Symbols

ε = convergence criterion
η = learning rate

Subscripts and Superscripts

i = inside
I = internal sources
j = wall number
m = step number
n = number of walls
o = outside
V = ventilation and infiltration
W = walls

References

[1] Pérez-Lombard, L., Ortiz, J., and Pout, C., 2008, "A Review on Buildings Energy Consumption Information," Energy Build., **40**(3), pp. 394–398.
[2] Chua, K. J., Chou, S. K., Yang, W. M., and Yan, J., 2013, "Achieving Better Energy-Efficient Air Conditioning—A Review of Technologies and Strategies," Appl. Energy, **104**, pp. 87–104.
[3] Hovgaard, T., Larsen, L., Skovrup, M., and Jørgensen, J., 2011, "Power Consumption in Refrigeration Systems—Modeling for Optimization," 4th International Symposium on Advanced Control of Industrial Processes, Hangzhou, May 23–26, pp. 234–239.
[4] Farrington, R., and Rugh, J., 2000, "Impact of Vehicle Air-Conditioning on Fuel Economy, Tailpipe Emissions, and Electric Vehicle Range," Earth Technologies Forum, National Renewable Energy Laboratory, Golden, CO, Report No. NREL/CP-540-28960.
[5] Farrington, R., Cuddy, M., Keyser, M., and Rugh, J., 1999, "Opportunities to Reduce Air-Conditioning Loads Through Lower Cabin Soak Temperatures," 16th International Electric Vehicle Symposium, Beijing, Oct. 12–16, Report No. NREL/CP-540-26615.
[6] Haines, R., and Hittle, D., 2006, *Control Systems for Heating, Ventilating, and Air Conditioning*, 6th ed., Springer, New York.
[7] Khayyam, H., Nahavandi, S., Hu, E., Kouzani, A., Chonka, A., Abawajy, J., Marano, V., and Davis, S., 2011, "Intelligent Energy Management Control of Vehicle Air Conditioning Via Look-Ahead System," Appl. Therm. Eng., **31**(16), pp. 3147–3160.
[8] Khayyam, H., 2013, "Adaptive Intelligent Control of Vehicle Air Conditioning System," Appl. Therm. Eng., **51**(1–2), pp. 1154–1161.
[9] Arguello-Serrano, B., and Velez-Reyes, M., 1999, "Nonlinear Control of a Heating, Ventilating, and Air Conditioning System With Thermal Load Estimation," IEEE Trans. Control Syst. Technol., **7**(1), pp. 56–63.
[10] Afram, A., and Janabi-Sharifi, F., 2015, "Gray-Box Modeling and Validation of Residential HVAC System for Control System Design," Appl. Energy, **137**, pp. 134–150.
[11] Zhu, Y., Jin, X., Fang, X., and Du, Z., 2014, "Optimal Control of Combined Air Conditioning System With Variable Refrigerant Flow and Variable Air Volume for Energy Saving," Int. J. Refrig., **42**, pp. 14–25.
[12] Qureshi, T., and Tassou, S., 1996, "Variable-Speed Capacity Control in Refrigeration Systems," Appl. Therm. Eng., **16**(2), pp. 103–113.
[13] ASHRAE, 1988, *Handbook of Fundamentals*, SI ed., American Society of Heating, Refrigerating and Air-Conditioning, Atlanta, GA.
[14] Barnaby, C. S., Spitler, J. D., and Xiao, D., 2005, "The Residential Heat Balance Method for Heating and Cooling Load Calculations," ASHRAE Trans., **111**(1), pp. 308–319.
[15] Fayazbakhsh, M. A., and Bahrami, M., 2013, "Comprehensive Modeling of Vehicle Air Conditioning Loads Using Heat Balance Method," SAE Technical Paper No. 2013-01-1507.
[16] Arici, O., Yang, S., Huang, D., and Oker, E., 1999, "Computer Model for Automobile Climate Control System Simulation and Application," Int. J. Appl. Thermodyn., **2**(2), pp. 59–68.
[17] Khayyam, H., Kouzani, A. Z., and Hu, E. J., 2009, "Reducing Energy Consumption of Vehicle Air Conditioning System by an Energy Management System," IEEE Intelligent Vehicles Symposium, Xi'an, China, June 3–5, pp. 752–757.
[18] Li, Q., Meng, Q., Cai, J., Yoshino, H., and Mochida, A., 2009, "Predicting Hourly Cooling Load in the Building: A Comparison of Support Vector Machine and Different Artificial Neural Networks," Energy Convers. Manage., **50**(1), pp. 90–96.
[19] Kashiwagi, N., and Tobi, T., 1993, "Heating and Cooling Load Prediction Using a Neural Network System," International Joint Conference on Neural Networks, IJCNN'93, Nagoya, Japan, Oct. 25–29, Vol. 1, pp. 939–942.
[20] Ben-Nakhi, A. E., and Mahmoud, M. A., 2004, "Cooling Load Prediction for Buildings Using General Regression Neural Networks," Energy Convers. Manage., **45**(13–14), pp. 2127–2141.
[21] Sousa, J. M., Babuška, R., and Verbruggen, H. B., 1997, "Fuzzy Predictive Control Applied to an Air-Conditioning System," Control Eng. Pract., **5**(10), pp. 1395–1406.
[22] Yao, Y., Lian, Z., Liu, S., and Hou, Z., 2004, "Hourly Cooling Load Prediction by a Combined Forecasting Model Based on Analytic Hierarchy Process," Int. J. Therm. Sci., **43**(11), pp. 1107–1118.
[23] Solmaz, O., Ozgoren, M., and Aksoy, M. H., 2014, "Hourly Cooling Load Prediction of a Vehicle in the Southern Region of Turkey by Artificial Neural Network," Energy Convers. Manage., **82**, pp. 177–187.
[24] Fayazbakhsh, M. A., Bagheri, F., and Bahrami, M., 2015, "An Inverse Method for Calculation of Thermal Inertia and Heat Gain in Air Conditioning and Refrigeration Systems," Appl. Energy, **138**, pp. 496–504.
[25] Wang, S., and Xu, X., 2006, "Parameter Estimation of Internal Thermal Mass of Building Dynamic Models Using Genetic Algorithm," Energy Convers. Manage., **47**(13–14), pp. 1927–1941.
[26] Wang, S., and Xu, X., 2006, "Simplified Building Model for Transient Thermal Performance Estimation Using GA-Based Parameter Identification," Int. J. Therm. Sci., **45**(4), pp. 419–432.
[27] Zhai, Z., Chen, Q., Haves, P., and Klems, J. H., 2002, "On Approaches to Couple Energy Simulation and Computational Fluid Dynamics Programs," Build. Environ., **37**(8–9), pp. 857–864.
[28] Zhai, Z., and Chen, Q., 2003, "Impact of Determination of Convective Heat Transfer on the Coupled Energy and CFD Simulation for Buildings," 8th International IBPSA Conference: Building Simulation, Eindhoven, The Netherlands, Aug. 11–14, pp. 1467–1474.
[29] Zhai, Z., Chen, Q., Klems, J. H., and Haves, P., 2001, "Strategies for Coupling Energy Simulation and Computational Fluid Dynamics Programs," 7th International IBPSA Conference, Rio de Janeiro, Aug. 13–15, pp. 59–66.
[30] Zhai, Z., and Chen, Q., 2003, "Solution Characters of Iterative Coupling Between Energy Simulation and CFD Programs," Energy Build., **35**(5), pp. 493–505.

[31] Zhai, Z., and Yan Chen, Q., 2004, "Numerical Determination and Treatment of Convective Heat Transfer Coefficient in the Coupled Building Energy and CFD Simulation," Build. Environ., **39**(8), pp. 1001–1009.
[32] Zhai, Z. J., and Chen, Q. Y., 2005, "Performance of Coupled Building Energy and CFD Simulations," Energy Build., **37**(4), pp. 333–344.
[33] Incropera, F. P., Lavine, A. S., and DeWitt, D. P., 2011, *Fundamentals of Heat and Mass Transfer*, Wiley, New York.
[34] Lippmann, R. P., 1988, "An Introduction to Computing With Neural Nets," ACM SIGARCH Comput. Archit. News, **16**(1), pp. 7–25.
[35] Liang, J., and Du, R., 2005, "Thermal Comfort Control Based on Neural Network for HVAC Application," IEEE Conference on Control Applications, CCA 2005, Toronto, ON, Aug. 28–31, pp. 819–824.
[36] Mehrotra, K., Mohan, C., and Ranka, S., 1997, *Elements of Artificial Neural Networks*, MIT Press, Cambridge, MA.
[37] Khayyam, H., Kouzani, A. Z., Hu, E. J., and Nahavandi, S., 2011, "Coordinated Energy Management of Vehicle Air Conditioning System," Appl. Therm. Eng., **31**(5), pp. 750–764.
[38] Arora, J., 2004, *Introduction to Optimum Design*, 2nd ed., McGraw-Hill, New York.